JOC Article
pubs.acs.org/joc

Chiral Conducting Surfaces via Electrochemical Oxidation of L-Leucine-Oligothiophenes

Christopher D. McTiernan, Karim Omri, and M'hamed Chahma*

Department of Chemistry & Biochemistry, Laurentian University, Sudbury, ON P3E 2C6, Canada

mchahma@laurentian.ca

Received April 22, 2010

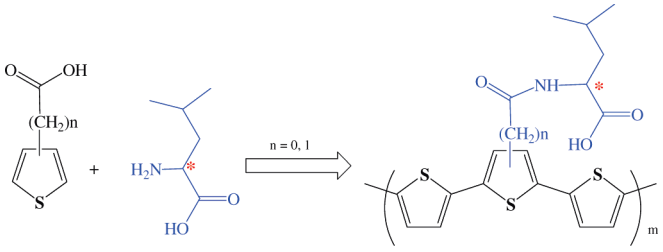

Polythiophenes bearing a specific chiral center such as L-leucine have been prepared via the electrochemical oxidation of a series of L-leucine functionalized oligothiophenes (monothiophenes and terthiophenes). These oligothiophenes have been prepared through the condensation of L-leucine methyl ester and the corresponding thiophene monomers in the presence of hydroxybenzotriazole (HOBt) and *N*,*N*′-dicyclohexylcarbodiimide (DCC) followed by hydrolysis of the esters. The electroactive polymers are electrochemically stable and exhibit excellent adhesive properties on electrode surfaces (platinum, gold, and glassy carbon) as well as interesting optical properties in both doped and undoped states. Hydrogen bonds between a free amino acid (L-leucine, D-leucine, L-alanine, D-alanine, and D/L-alanine) and the L-leucine based polythiophenes (*chiral conducting surface*) were probed using cyclic voltammetry. Preliminary results show that the capacitive current of a modified L-leucine-polythiophene electrode decreases as a result of the formation of a hydrogen bond barrier on the surface of the *chiral conducting surface* accompanied with a shift of the oxidation potential. Cyclic voltammetry responses resulting from the interaction of the *chiral conducting surface* with L and D free amino acid isomers are similar. The formation of hydrogen bonds between the *chiral conducting surface*s and the free amino acids was characterized by ^{1}H NMR. A chemical shift was observed for the N−H group in monomer **6** as a result of the hydrogen bond formation between the L-leucine methyl ester (D-leucine methyl ester, D/L-leucine methyl ester) and monomer **6**.

Introduction

There have been numerous methods utilized to immobilize bioorganic molecules such as oligonucleotides and peptides onto solid conducting surfaces for recognition purposes.[1,2] At the moment one of the most common immobilization techniques involves the use of modified biomolecules that contain a sulfur linker, which binds strongly to gold.[3,4] By reduction of aryl diazonium salts, other organic molecules

(1) (a) Huang, E.; Zhou, F.; Deng, L. *Langmuir* **2000**, *16*, 3272–3280. (b) Mucic, R. C.; Herrlein, M. K.; Mirkin, C. C.; Letsinger, R. L. *Chem. Commun.* **1996**, 555–557. (c) Yu, J.; Wang, H.; Wan, Y.; Yomanto, H.; Kim, J. C.; Donilon, L. H.; Tao, C.; Strong, M.; Choing, Y. *J. Org. Chem.* **2001**, *66*, 2937–2942. (d) Long, Y.-T.; Li, C.-Z.; Sutherland, T. C.; Chahma, M.; Lee, J. S.; Kraatz, H.-B. *J. Am. Chem. Soc.* **2003**, *125*, 8724–8725. (e) Meade, T. J.; Kayyem, J. F. *Angew. Chem. Int. Engl.* **1995**, *34*, 352–354.

(2) (a) Kertesz, V.; Whittemore, N. A.; Inamati, G. B.; Manoharan, M.; Cook, P. D.; Baker, D. C.; Chambers, J. Q. *Electroanalysis* **2000**, *12*, 889–884. (b) Kim, J.; Cho, J.; Seidler, P. M.; Kurland, N. E.; Yadavalli, V. K. *Langmuir* **2010**, *26*, 2599–2608. (c) Kelley, S. O.; Boon, E. M.; Barton, J. K.; Jackson, N. M.; Hill, M. G. *Angew. Chem., Int. Ed.* **1999**, *38*, 941–945.

(3) (a) Kelly, S. O.; Barton, J. K.; Jackson, N. M.; Hill, M. G. *Bioconjugate Chem.* **1997**, *8*, 31–37. (b) Chahma, M.; Lee, J. S.; Kraatz, H.-B. *J. Electroanal. Chem.* **2004**, *567*, 283–287. (c) Herne, T. K.; Tarlov, M. J. *J. Am. Chem. Soc.* **1997**, *119*, 8916–8920. (d) Kelley, S. O.; Barton, J. K.; Jackson, N. M.; McPherson, L. D.; Potter, A. B.; Spain, E. M.; Allen, M. J.; Hill, M. G. *Langmuir* **1998**, *14*, 6781–6784.

(4) (a) Plumb, K.; Kraatz, H.-B. *Bioconjugate Chem.* **2003**, *4*, 601–606. (b) Hager., G.; Brolo, A. G. *J. Electroanal. Chem.* **2003**, *550−551C*, 291–301.

Published on Web 08/18/2010 DOI: 10.1021/jo100722v

have also been grafted onto glassy carbon electrodes.[5,6] However, problems with reproducibility that result from difficulties preparing the surface of gold electrodes as well as the presence of phosphates, alcohols, and amines that may perturb the adsorption process hinder this immobilization process.[7] To prevent some of these problems, it has been reported that layers of conducting material could be used as an interface between biomolecule probes and electrode surfaces, which will facilitate the immobilization and sensing of the desired molecules.[8]

Polythiophenes and other π-conjugated polymers appear to be ideal for such purposes because of their (i) excellent adhesion properties to the surface of electrodes, (ii) stability in both the doped and dedoped states, (iii) well-known electrochemical oxidation of their monomers, and (iv) ability to carry functionalities that can be exploited for biomolecule immobilization.[9,10]

π-Conjugated polymers such as cationic poly(fluorene-*co*-phenylene) have been employed to discriminate DNA strands via amplification of the optical signal resulting from the electrostatic interactions between DNA strands and the charged polymer.[11] Cationic polythiophenes have also been used in the same way to detect nucleic acids and proteins via fluorescence and electrochemical responses, respectively.[12] Moreover, optically active functionalized polythiophenes have been prepared using either chemical ($FeCl_3$ as oxidizing agent) or electrochemical (oxidation of the monomer on platinum electrode) oxidations.[13]

CHART 1. Monothiophene and Terthiophene Bearing Amino Acids

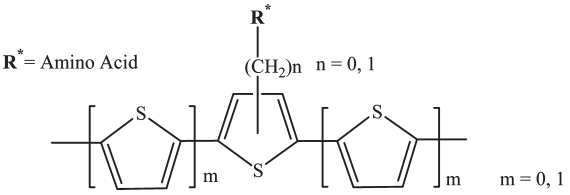

Our strategy toward the detection of biomolecules is to take advantage of the electrical conductivity and optical properties of polythiophenes to prepare a *chiral conducting surface* via electrochemical oxidation of the chiral oligomers. We recently reported the synthesis and characterization of several oligothiophenes bearing D/L-alanine, and their corresponding polymers.[14] The latter exhibit excellent stability in both states. However, these polymers have no specific chirality, which may limit their use to recognize specific target molecules. A design of new polythiophenes bearing specific chiral center such as L-leucine may overcome this limitation. This approach requires the synthesis of L-leucine-oligothiophenes (Chart 1), which after electrochemical oxidation will afford a conducting surface with pendant chiral centers. The *chiral conducting surface* will display several advantages such as the ability to be regenerated by controlling the thickness of the deposited film layers and to recognize specific motifs.

Herein, we present (i) the synthesis and characterization of a variety of oligo/polythiophenes bearing L-leucine amino acid, (ii) electrochemical property of the polymers, and (iii) preliminary results of the hydrogen bond interactions of the *chiral conducting surface* with other amino acids.

Results and Discussion

The synthetic route for monothiophenes and terthiophenes bearing an amino acid with a specific chiral center such as L-leucine is summarized in Scheme 1. The condensation of either thiophene carboxylic acid or thiophene acetic acid with L-leucine methyl ester in the presence of hydroxybenzotriazole (HOBT) and *N*,*N*′-dicyclohexylcarbodiimide (DCC) affords compounds **3** and **4** which were then hydrolyzed to the desired compounds **5** and **6** (Scheme 1A). A similar methodology was employed for the preparation of compounds **9**, **10**, **13** and **14**. However, a cross coupling reaction[15] (Stille coupling) using tetrakistriphenylphosphine-Palladium (0) as the catalyst was necessary to produce the terthiophene oligomers **11** and **12** (Scheme 1B). The specific chiral center of L-leucine is attached to the mono/terthiophene via a carbonyl group (oligomers with $n = 0$) or an alkyl group (oligomers with $n = 1$). In addition to the high yield of the reactions and their stability in the presence of

(5) (a) Adenier, A.; Combellas, C.; Kanoufi, F.; Pinson, J.; Podvorica, F. I. *Chem. Mater.* **2006**, *18*, 2021–2029. (b) Gallardo, I.; Pinson, J.; Vilà., N. *J. Phys. Chem. B* **2006**, *110*, 19521–19529. (c) Combellas, C.; Kanoufi, F.; Pinson, J.; Podvorica, F. I. *J. Am. Chem. Soc.* **2008**, *130*, 8576–8577.

(6) (a) Coulon, E.; Pinson, J.; Bourzat, J.-D.; Commerçon, A.; Pulicani, J.-P. *J. Org. Chem.* **2002**, *67*, 8513–8518. (b) Baranton, S.; Bélanger, D. *J. Phys. Chem. B* **2005**, *109*, 24401–24410. (c) Tan, S.; Bélanger, D. *J. Phys. Chem. B* **2005**, *109*, 23480–23490.

(7) Kimura-Suda, H.; Petrovykh, D. Y.; Tarlov, M. J.; Whitman, L. J. *J. Am. Chem. Soc.* **2003**, *125*, 9014–9015.

(8) (a) Rahman, M. A.; Kwon, N.-H.; Won, M.-S.; E. S. Choe, E. S.; Shim, Y.-B. *Anal. Chem.* **2005**, *77*, 4854–4860. (b) Kim, H.-J.; Lee, K.-S.; Won, M.-S. ; Shim, Y.-B. *Langmuir* **2008**, *24*, 1087–1093. (c) Konry, T.; Novoa, A.; Shemer-Avni, Y.; Hanuka, N.; Cosnier, S.; Lepellec, A.; Marks, R. S. *Anal. Chem.* **2005**, *77*, 1771–1779. (d) Gooding, J. J.; Wasiowych, C.; Barnett, D.; Hibbert, D. B.; Barisci, J. N.; Wallace, G. G. *Biosens. Bioelectron.* **2004**, *20*, 260–268.

(9) (a) Roncali, J. *Chem. Rev.* **1992**, *92*, 711–738. (b) Groenendaal, L.; Jonas, F.; Freitag, D.; Pielartzik, H.; Reynolds, J. R. *Adv. Mater.* **2000**, *12*, 481–534. (c) Groenendaal, L.; Zotti, G.; Aubert, P. H.; Waybright, S. M.; Reynolds, J. R. *Adv. Mater.* **2003**, *15*, 855–879. (d) Clot, O.; Wolf, M. O.; Patrick, B. O. *J. Am. Chem. Soc.* **2001**, *123*, 9963–9973.

(10) (a) Wolf, M. O. *Adv. Mater.* **2001**, *13*, 545–553. (b) Zhou, Q.; Swager, T. M. *J. Am. Chem. Soc.* **1995**, *117*, 12593–12602. (c) McQuade, D. T.; Pullen, A. E.; Swager, T. M. *Chem. Rev.* **2000**, *100*, 2537–2574. (d) McCullough, R. D. *Adv. Mater.* **1998**, *10*, 93–116. (e) Fichou, D. *Handbook of Oligo- and Polythiophenes*; Wiley-VCH: Weinheim, 1999.

(11) (a) Liu, B.; Bazan, G. C. *J. Am. Chem. Soc.* **2004**, *126*, 1942–1943. (b) Liu, B.; Bazan, G. C. *J. Am. Chem. Soc.* **2006**, *128*, 1188–1196. (c) Liu, B.; Bazan, G. C. *Chem. Mater.* **2004**, *16*, 4467–4476.

(12) (a) Ho, H. A.; Boissinot, M.; Bergeron, M. G.; Corbeil, G.; Doré, K.; Boudreau, D.; Leclerc, M. *Angew. Chem., Int. Ed.* **2002**, *41*, 1548–1551. (b) Ho, H.-A.; Leclerc, M. *J. Am. Chem. Soc.* **2003**, *125*, 4412–4413. (c) Ho, H.-A.; Leclerc, M. *J. Am. Chem. Soc.* **2004**, *126*, 1384–1387. (d) Doré, K.; Dubus, S.; Ho, H.-A.; Lévesque, I.; Corbeil, G.; Boissinot, M.; Boivin, G.; Bergeron, M. G.; Boudreau, D.; Leclerc, M. *J. Am. Chem. Soc.* **2004**, *126*, 4240–4244. (e) Le Floch, F.; Ho, H.-A.; Leclerc, M. *Anal. Chem.* **2006**, *78*, 4727–4731.

(13) (a) Nilsson, K. P. R.; Andersson, M. R.; Inganas, O. *Synth. Met.* **2003**, *135*−*136*, 291–292. (b) Nilsson, K. P. R.; Johan, D.; Olsson, J. D.; Konradsson, P.; Inganas., O. *Macromolecules* **2004**, *37*, 6316–6321. (c) Nilsson, K. P. R.; Olsson, J. D.; Stabo-Eeg, F.; Lindgren, M.; Konradsson, P.; Inganas, O. *Macromolecules* **2005**, *38*, 6813–6821. (d) Goto, H.; Yashima, E. *J. Am. Chem. Soc.* **2002**, *124*, 7943–7949. (e) Yashima, E.; Goto, H.; Okamoto, Y. *Macromolecules* **1999**, *32*, 7942–7945. (f) Goto, H.; Okamoto, Y.; Yashima, E. *Chem.—Eur. J.* **2002**, *8*, 4027–4036. (g) Lemaire, M.; Delabouglise, D.; Garreau, R.; Guy, A.; Roncali, J. *Chem. Commun.* **1988**, 658–661. (h) Caras-Quintero, D.; Bäuerle, P. *Chem. Commun.* **2004**, 926–927. (i) Caras-Quintero, D.; Bäuerle, P. *Chem. Commun.* **2002**, 2690–2691. (j) Pellon, P.; Deltel, E.; Pilard, J.-F. *Tetrahedron Lett.* **2001**, *42*, 867–869. (k) Grenier, C.R. G.; George, S. J.; Joncheray, T. J.; Meijer, E. W.; Reynolds, J. R. *J. Am. Chem. Soc.* **2007**, *129*, 10694–10699.

(14) McTiernan, C. D.; Chahma, M. *New J. Chem.* **2010**, *34*, 1417–1423.

(15) (a) Stille, J. K. *Angew. Chem., Int. Ed. Engl.* **1986**, *25*, 508–524. (b) Stille, J. K. *Pure Appl. Chem.* **1985**, *57*, 1771–1780. (c) Chahma, M.; Gilroy, J. B.; Hicks, R. G. *J. Mater. Chem.* **2007**, *17*, 4768–4771. (d) Schwab, P. F. H.; Fleischer, F.; Michl, J. *J. Org. Chem.* **2002**, *67*, 443–449.

SCHEME 1. Synthetic Pathway for Amino Acid Functionalized Monothiophenes (A) and Terthiophenes (B)

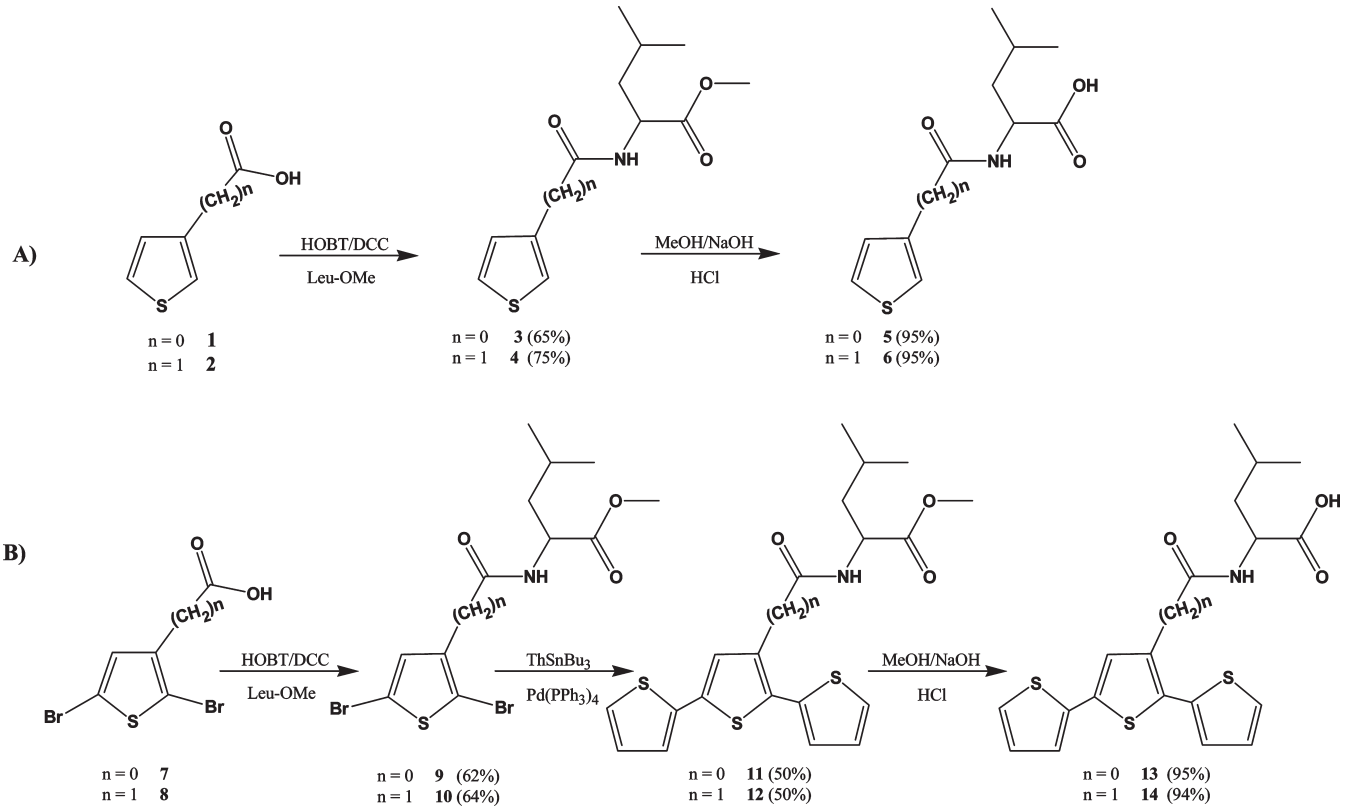

organic solvents and moisture, the newly prepared oligothiophenes have the positions 2,5 unsubstituted to allow the chemical or electrochemical polymerization to occur.[16]

TABLE 1. Electrochemical and Optical Properties of Prepared L-Leucine-oligothiophenes and Their Corresponding Polymers in ACN; First Scan Using 0.1 V/s Scan Rate

compounds	λ_{max} (nm)	E_p or $[E_{1/2}]$ (V vs Fc^+/Fc) ± 0.02 V
3	251	
4	261	
5	242	
6	235	
11	348	0.830
12	342	0.660
13	344	0.880
14	342	0.670
poly(**11**)-*Pt*	468[a]/634[b]	[0.510]
poly(**12**)-*Pt*	466[a]/623[b]	[0.400]
poly(**13**)-*Pt*	464[a]/646[b]	[0.480]
poly(**14**)-*Pt*	451[a]/662[b]	[0.410]

[a]Undoped polymer. [b]Doped polymer.

Cyclic voltammetry (CV) and linear sweep voltammetry (LSV) were used to investigate the redox properties of the prepared L-leucine functionalized oligothiophenes. As is typical for 2,5-unsubstituted oligothiophenes, an irreversible oxidation wave was observed due to the electropolymerization process via radical cation-radical cation coupling to form a carbon−carbon bond. The oxidation peak potential of all irreversible systems is summarized in Table 1. The oxidation peak potential of the monomers **3**−**6** was not reported because it was outside of the potential window of the solvent/supporting electrolyte system.

Upon examination of the oxidation peak potential of the monomers, two trends are noticeable. The first is that monomers with a methylene linker exhibit lower oxidation potentials than those without, which can be attributed to the electro-donating behavior of this substituent.[17] The second trend is that the terthiophene monomers exhibit a lower oxidation potential than the monothiophenes.[18] This can be explained by the increase in the degree of conjugation in the terthiophenes, which results in the electronic delocalization of the π-system.

L-Leucine functionalized terthiophenes were successfully electropolymerized in a 1 M n-Bu_4NPF_6/ACN solution through repeated CV cycling beyond the oxidation peak potential of the thiophene component of each monomer for **12** (0.660 V vs Fc^+/Fc) and **14** (0.670 V vs Fc^+/Fc). The 10 scan electropolymerization CVs of compounds **12** and **14** are presented in Figure 1 (left). An increase of the peak current with each successive scan was observed during the oxidation process, which is due to the deposition of a polymer film layer (poly(**12**) and poly(**14**)) on the surface of the platinum electrode (gold and glassy carbon).

In order to study the stability and electrochemical properties of the deposited films, poly(**11**−**14**)-*Pt* were then placed in a fresh solution of monomer free ACN/supporting electrolyte. For all deposited polymers, the peak current varies

(16) (a) Tourillon, G.; Garnier, F. *J. Electroanal. Chem.* **1982**, *135*, 173–178. (b) Roncali, J.; Garnier., F. *J. Phys. Chem.* **1988**, *92*, 833–840.

(17) Brillas, E.; Oliver, R.; Estrany, F.; Rodriguez, E.; Tejer, S. *Electrochim. Acta* **2002**, *47*, 1623–1631.

(18) (a) Hicks, R. G.; Nodwell, M. B. *J. Am. Chem. Soc.* **2000**, *122*, 6746–6753. (b) Bednarz, M.; Reineker, P.; Osteritz, E.-M.; Bäuerle, P. *J. Lumin.* **2004**, *110*, 225–231.

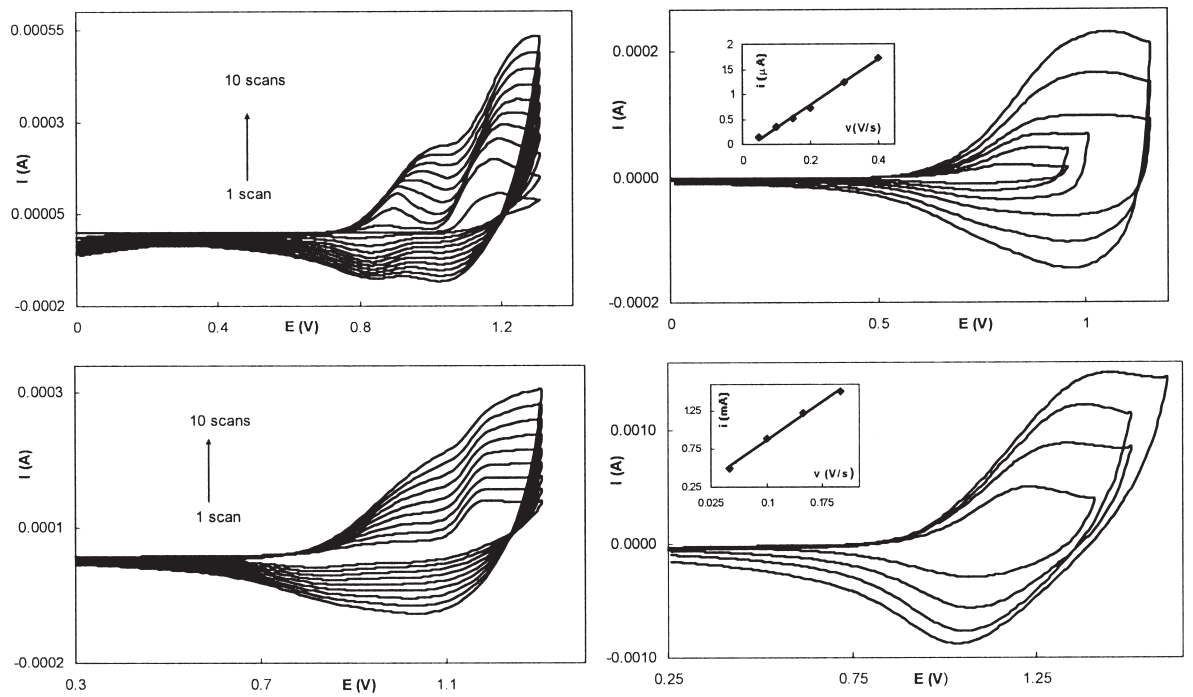

FIGURE 1. A 10 scan electrochemical oxidation of **12** (top left) and **14** (bottom left) in ACN (scan rate = 0.1 V/s; WE = platinum electrode; RE = silver wire; CE = platinum wire) and CV of their corresponding polymer poly(**12**)-*Pt* (top right) and poly(**14**)-*Pt* (bottom right) at different scan rates.

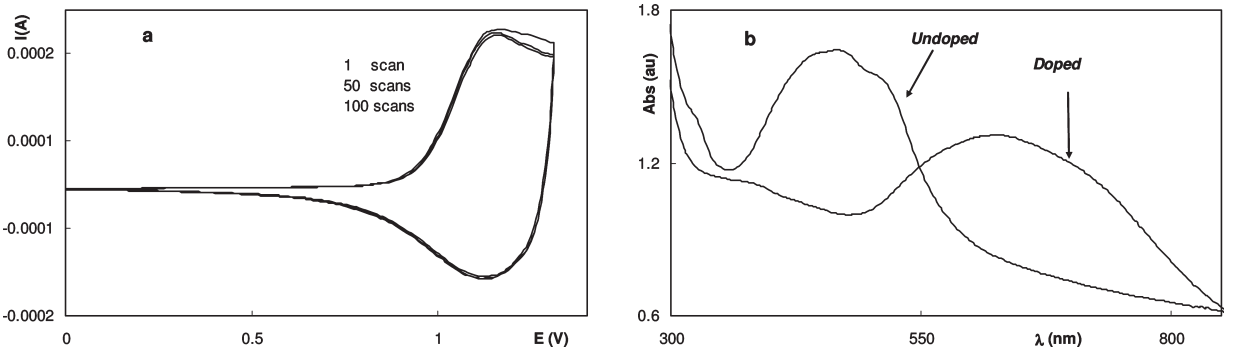

FIGURE 2. (a) Stability curve of poly(**12**)-*Pt*. (b) UV−vis spectra of poly(**12**)-*ITO* in both the doped (blue) and undoped (orange) states.

linearly with the scan rate (0.05−0.40 V/s) indicating a surface bound species (Figure 1, right for poly(**12** and **14**)-*Pt*), whereas in solution the peak current varies linearly with the square root of the scan rate.[19]

Moreover, these films are stable over 100 CV scans with a scan rate of 0.1 V/s. As shown in Figure 2a, poly(**12**)-*Pt* displays excellent stability in both states doped and undoped and is fully reversible. The peak current remains constant and no significant change or degradation of their electrochemical behavior was observed over 100 CV scans. The $E_{1/2}$ (average of oxidation and reduction peak potentials) of all polymers is recorded in Table 1.

The optical properties of the monomers and their corresponding polymers were examined. The differences seen relate back to the length of conjugation and the electro-donating/withdrawing behavior of the different substituents.[18] The absorption maxima of the monomers and corresponding polymers (in both the doped and undoped states) are recorded in Table 1. The presence of a methylene or a carbonyl group on either mono- or terthiophenes has no significant effect on the λ_{max}. On the other hand, the absorption maximum of the terthiophenes is red-shifted in comparison to the monothiophenes, which is due to the increase of conjugation length in terthiophenes.[20]

The insolubility of the polymers in commonly used organic solvents made classical optical characterization techniques difficult. Through the use of an indium tin oxide (ITO) electrode, UV−vis spectra of the deposited films were obtained. The polymers were deposited on the ITO electrode by controlled potential electrolysis (beyond the oxidation peak potential of the monomer) using a platinum plate as the

(19) Bard, A. J.; Faulkner, L. R. *Electrochemical Methods. Fundamentals and Applications*, 2nd ed.; Wiley: New York, 2001.

(20) (a) Brillas, E.; Oliver, R.; Estrany, F.; Rodriguez, E.; Tejer, S. *Electrochim. Acta* **2002**, *47*, 1623–1631. (b) Roncali, J.; Garnier, F.; Lemaire, M.; Gerreau, R. *Synth. Met.* **1986**, *15*, 323–331.

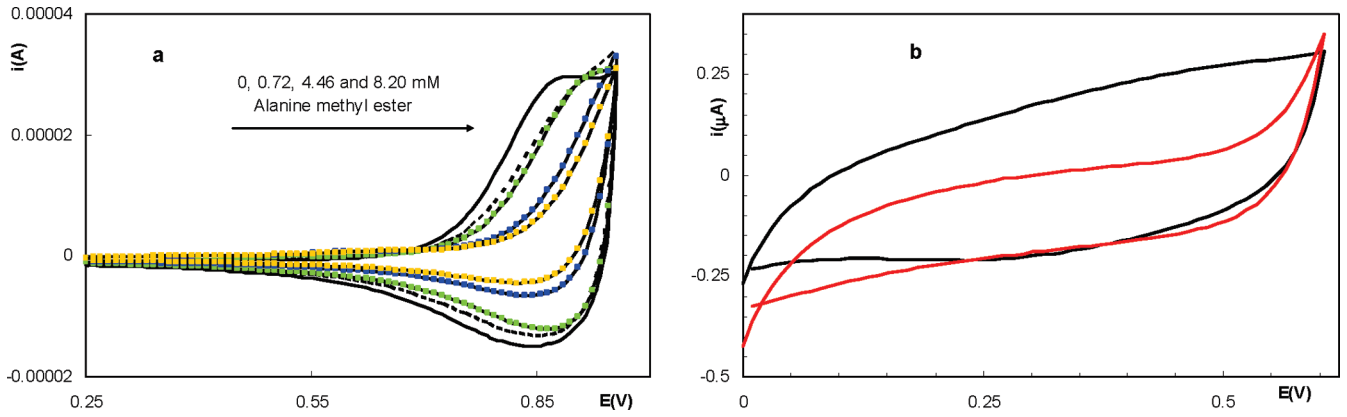

FIGURE 3. (a) Interactions between poly(**14**)-*Pt* with D/L-alanine methyl ester. (b) Capacitive current of poly(**14**)-*Pt* in the absence (black) and presence (orange) of D/L-alanine methyl ester.

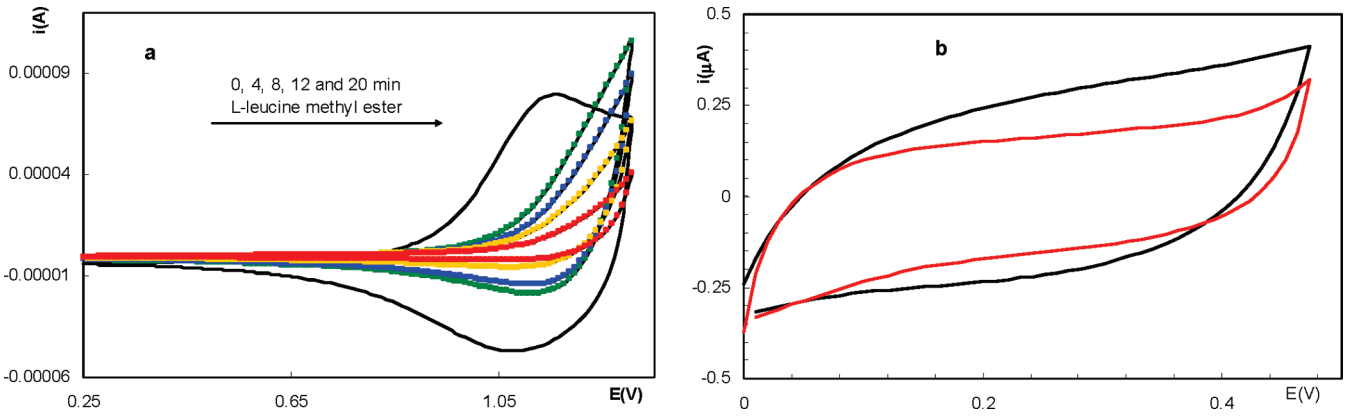

FIGURE 4. (a) Interactions between poly(**14**)-*Pt* with L-leucine methyl ester (1.87×10^{-3} M). (b) Capacitive current of poly(**14**)-*Pt* in the absence (black) and presence (orange) of L-leucine methyl ester.

cathode and the ITO electrode as the anode. Figure 2b represents the UV−vis spectra of poly(**11**)-*ITO* in both states. Poly(**11**−**14**)-*ITO* showed similar UV−vis behavior; they are dark blue in their doped form and orange in their undoped form. Poly(**11**−**14**)-*Pt* have been also characterized using ATR-IR. Poly(**11**)-*Pt* and poly(**12**)-*Pt* exhibit characteristic stretches corresponding to the carbonyl of the ester (1743 cm^{-1}) and the carbonyl of the amide (1666 cm^{-1}). For poly(**13**)-*Pt* and poly(**14**)-*Pt*, in addition to the amide stretch, the carbonyl of the carboxylic acid appears at 1731 cm^{-1} (see Supporting Information).

For recognition purposes, the first attempt to probe the hydrogen bond formation on the *chiral conducting surface* was carried out using L-leucine methyl ester or D/L-alanine methyl ester. After deposition of the polymer (poly(**14**)-*Pt*) and verification of its electrochemical and adhesive stability over 100 scans, a few CVs were performed of the modified electrode in the presence of various concentrations of D/L-alanine methyl ester (0.072×10^{-3}−8.20×10^{-3} M). As depicted in Figure 3a, a potential shift was observed with the increase of the concentration of the amino acid. This behavior is due to the formation of a hydrogen bond barrier at the surface of the deposited film causing a decrease in the electron transfer constant through the *chiral conducting surface*.

Similar behavior has been described for conducting materials bearing mimic DNA nucleobases.[21] A deposited diamino pyrimidine substituted poly(bithiophene) on platinum electrode using electrochemical oxidation shows in cyclic voltammetry a decrease in the oxidation peak current and a shift of the oxidation peak potential once interactions with a free uracil occur. This behavior is due to the formation of a hydrogen bond barrier at the surface of the deposited film causing a decrease in the electron transfer constant through the *chiral conducting surface*. The hydrogen bonding prevents the penetration of the ions from the supporting electrolyte, which results in the loss of the electroactivity of the conducting polymer therefore creating a barrier. The loss of the electroactivity depends on the strength of the base pair formations. More ions are trapped when the hydrogen bonds between base pairs are stronger, and significant loss of the electroactivity of the conducting surface is observed.

The potential shift can be recovered partially by placing the *chiral conducting surface*-D/L-alanine methyl ester in a new free amino acid fresh solution (Figure 3a dashed line).

In the case of the hydrogen bond interactions with L-leucine methyl ester (1.87×10^{-3} M), the decrease in the oxidation peak current and the potential shift of poly(**14**)-*Pt* (Figure 4a) is accompanied by a significant decrease in the nonfaradaic current (capacitive current, Figure 4b). Poly-(**14**)-*Pt*/L-leucine methyl ester hydrogen bonds are stronger

(21) (a) Emge, A.; Bäuerle, P. *Synth. Met.* **1999**, *102*, 1370–1373. (b) Bäuerle, P.; Emge, A. *Adv. Mater.* **1998**, *10*, 324–330.

than the ones observed with D/L-alanine methyl ester, which may explain the inability to recover the current and the potential in the case of the interaction between poly(**14**)-*Pt* and L-leucine methyl ester. Via theoretical calculation for peptides, it was reported that leucine−leucine interactions are stronger than leucine-alanine.[22]

The capacitive current of the *chiral conducting surface* (Poly(**14**)-*Pt*) decreases by almost 50% once interacting with L-leucine methyl ester (Figure 4b). The capacitive current depends on the concentration of the supporting electrolyte. As hydrogen bonds form at the surface of the *chiral conducting surfaces* after addition of the free amino acid, ions of the supporting electrolyte are trapped and cause a decrease in the capacitive current. This behavior has also been seen for poly(**14**)-*Pt* in the presence of D/L-alanine methyl ester (Figure 3b). For poly(**14**)-*Pt*/L-leucine methyl ester pairs, different concentrations of free L-leucine methyl ester have been examined and afford the same results as presented above for 1.87×10^{-3} M. A control CV of poly(terthiophene)-*Pt* was performed in the presence of D/L-alanine methyl ester and L-leucine methyl ester (see Supporting Information). The peak current and the potential of the unsubstituted poly(terthiophene)-*Pt* remained constant, which demonstrates that the interactions of the *chiral conducting surface* in poly(**14**)-*Pt* with other amino acids via hydrogen bond formation.

The interaction of the *chiral conducting surface* poly(**14**)-*Pt* with other free chiral amino acids such as D-leucine methyl ester, D/L-leucine methyl ester, D-alanine methyl ester, and L-alanine methyl ester has been investigated and shows a behavior identical to the one observed with poly(**14**)-*Pt*/L-leucine methyl ester. It is noteworthy that in our case the nature of the chirality has no significant effect on the electrochemical responses using cyclic voltammetry. The latter is not sensitive enough to distinguish between the interaction of the *chiral conducting surface* with the D and L isomers of the amino acids. It was also reported that the chirality does not change the backbone of the polymer as it was stated by Nilsson et al.[13a−c] They found that (i) the absorption of both stereoisomeric-polymers was similar and (ii) the alteration of the stereochemistry of the side chain does not influence the absorption properties of the polymer.

To probe the hydrogen bond formations between the *chiral conducting surface* and a free amino acid, ^{1}H NMR of a thiophene monomer bearing a L-leucine (**6**) has been studied in deuteriated acetonitrile in the absence and presence of free L-leucine methyl ester. Figure 5 demonstrates that there is a chemical shift of the N−H (amide) group of compound **6** (20 mM) after adding 1 (20 mM) or 2 (40 mM) equiv of L-leucine methyl ester. This shows that the origin of the hydrogen bonds on *the chiral conducting surfaces* comes from the interaction of the chiral center attached to the conducting polymer and the free amino acid in solution. The chemical shift of the aromatic protons of the thiophene moiety remains constant after addition of one or two equivalents of L-leucine methyl ester. Moreover, a similar study was performed for monomer **6** with different concentrations of D-leucine methyl ester and D/L-leucine methyl ester. The ^{1}H NMR spectra showing the hydrogen bond formation are presented in the Supporting Information. The interaction of monomer **6** with free amino acid isomers D or L and the racemic mixture D/L was found to be identical.

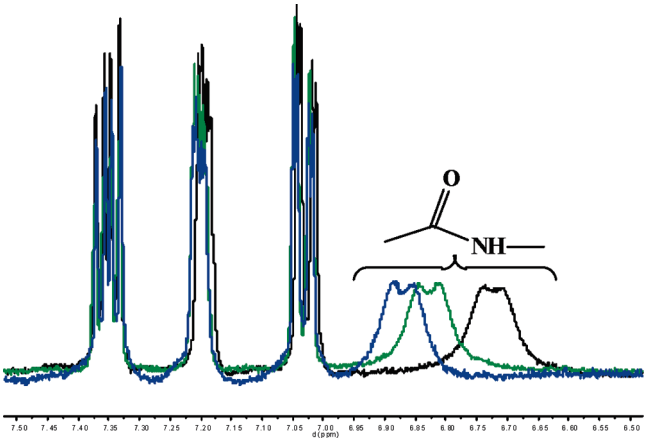

FIGURE 5. ^{1}H NMR of compound **6** (20 mM) in the absence (black) and in the presence of L-leucine methyl ester (1 equivalent: green; 2 equivalents: blue).

Summary

The synthesis of a variety of monoterthiophenes bearing L-leucine is reported. All these monomers are stable to moisture and organic solvents. The electrochemical oxidation of L-leucine functionalized terthiophenes affords polythiophenes with specific chirality (*chiral conducting surface*), which display excellent stability in both doped and undoped states and exhibit excellent adhesive properties on several electrodes (platinum, gold, and glassy carbon). Hydrogen bond formation between the *chiral conducting surface* and free amino acids such as L-leucine, D-leucine, D-alanine, L-alanine, and D/L-alanine has been probed using cyclic voltammetry. Preliminary results show that the potential of the electroactive species was shifted as result of the formation of a hydrogen bond barrier. Moreover, a drastic change in the capacitive current was observed. However, cyclic voltammetry responses (potential shift and current) were similar for the interactions between the *chiral conducting surfaces* and both L and D free amino acid isomers. Further investigations toward the characterization of the hydrogen bond formation with amino acids and peptides (proteins) using electrochemical methods such as surface plasmon resonance (SPR) to determine the capacitive current of the *chiral conducting surface* once interacting L or D free amino acids and impedance measurements to calculate the kinetic constants as well as theoretical calculations to estimate the energy of the hydrogen bond formations are currently underway.

Experimental Section

Generalities. Unless stated otherwise, all reactions and manipulations were carried out under an argon atmosphere. Glassware was oven-dried at 100 °C for 24 h prior to use. Solvents were dried using activated (24 h at 100 °C) molecular sieve (4 Å). All reagents were purchased from commercial sources and used as received except where stated otherwise. Compound **7** and **8** were prepared according to literature procedures.[14]

^{1}H-proton (^{13}C- carbon) NMR spectra were recorded on a 200 (50) MHz NMR spectrometer. The NMR samples were prepared from using ~20 mg of product dissolved in 1 mL of deuterated solvent (DMSO-d_6 or $CDCl_3$). IR spectra were recorded on a Fourier-transform infrared spectrophotometer.

(22) Lapointe, S. M.; Farrag, S.; Bohórquez, J.; Boyd, R. J. *J. Phys. Chem. B* **2009**, *113*, 10957–10964.

KBr pellet method was utilized to obtain all spectra of solid compounds with a ratio of (product/KBr) = 1/100. The NaCl disk method was employed to obtain the infrared spectra of the viscous liquid samples. For poly(**11**−**14**)-*Pt*, attenuated total reflection infrared (ATR-IR) was used. UV−vis spectra were recorded on a spectrophotometer.

The electrochemical experiments were performed using a potentiostat at room temperature (22 ± 2 °C). Voltammetric measurements were performed in acetonitrile (ACN) containing 1 M of n-Bu_4NPF_6. The platinum electrode (diameter 1.6 mm) was used as the working electrode. Platinum wire was used as auxiliary electrode and silver wire was used as reference electrode. All oxidation peak potentials are reported versus an internal reference ferrocene/ferrocenium redox (E^0 = 0.390 V vs AgCl/Ag, E^0 = 0.350 V vs SCE). The working electrode was polished on alumina before use. *iR* compensations were applied for all experiments. The bulk electrolyses were performed using a controlled potential in a cell with one compartment using a platinum plate (1.5 cm^2) and ITO electrode as the cathode and anode respectively. The imposed potential for the electrolysis of compounds **11**−**14** is 1.3 V (vs AgCl/Ag).

General Synthesis for 3, 4, 9, and 10. L-Leucine methyl ester hydrochloride (0.360 g, 2 mmol) and triethylamine (0.28 mL, 2 mmol) were added to 40 mL of anhydrous dichloromethane. After stirring for 1 h, this solution was added dropwise to a solution of 2,5-dibromothiophene carboxylic acid (0.572 g, 2 mmol), hydroxybenzotriazole (0.270 g, 2 mmol), and dicyclohexylcarbodiimide (0.410 g, 2 mmol) in 60 mL of anhydrous dichloromethane that had also been stirred for 1 h. The reaction was followed by TLC and was found to be complete after 24 h. After filtration to eliminate the dicyclohexylurea byproduct, the organic reaction mixture was washed 5 times with 100 mL of a $NaHCO_3$ saturated solution followed by five 100-mL washes with water. The organic phase was then dried over $MgSO_4$ and evaporated to dryness. The product was then purified via column chromatography on silica gel with specific eluent.

General Synthesis of 11 and 12. 2,5-Dibromo-thiophene-3-carbonyl-leucine methyl ester (0.5886 g, 1.49 mmol), 2-tributylstannyl-thiophene (1.11 mL, 2.98 mmol), and $Pd(Ph_3)_4$ (0.300 g, 0.255 mmol) were added to 25 mL of toluene, which had been dried over 4 Å molecular sieves and degassed for 1 h with N_2. The reaction mixture was allowed to stir for 48 h at 90 °C. The reaction was followed by TLC. Once complete the reaction mixture was filtered through Celite to remove the catalyst. The mixture was then washed five times with 100 mL of a cesium fluoride solution, followed by five 100-mL washes with water. The organic phase was then dried over $MgSO_4$ and evaporated to dryness. The crude product was then purified via column chromatography utilizing a solvent system of 30% ethyl acetate and 70% dichloromethane.

General Synthesis of 5, 6, 13, and 14. Terthiophene-3-leucine methyl ester (0.150 g, 3.70 mmol) and 1 N NaOH (2.2 mL) were added to 2 mL of methanol. The reaction mixture was then allowed to stir at room temperature for 3.5 h, after which 1 N HCl (1 mL) was added. The MeOH was then removed in vacuo and the remaining solution was cooled in an ice bath. 1 N HCl (2 mL) was then added dropwise to the solution, which was then allowed to cool in a refrigerator overnight. The desired product was then filtered off and dried under reduced pressure.

Synthesis of 4-Methyl-2-[(thiophene-3-carbonyl)-amino]-pentanoic Acid Methyl Ester (3). Product: white solid. The solvent used for the column chromatography on silica gel was ethyl acetate/CH_2Cl_2 (20/80, R_f = 0.67). Yield: 65%. Mp: 126 °C. ^{1}H NMR (200 MHz, $CDCl_3$) δ (ppm) 7.92−7.84 (m, 1H), 7.44−7.36 (m, 1H), 7.36−7.24 (m, 1H), 6.59 (s br, 1H), 4.92−4.76 (m, 1H), 3.79 (s, 3H), 1.90−1.52 (m, 3H), 1.12−0.88 (m, 6H). ^{13}C NMR (50 MHz, $CDCl_3$) δ (ppm) 174.0, 162.8, 137.1, 128.8, 126.6, 126.3, 52.5, 51.1, 42.1, 25.2, 23.0, 22.2. IR (KBr) υ (cm^{-1}) 1733 (CO ester), 1625 (CO amide). UV−vis (ACN) λ_{max} (ε) 251 nm (2.03×10^4 M^{-1} cm^{-1}). pHRMS (EI) for $C_{12}H_{17}NO_3S$ [M^+]: calcd 255.0924; found 255.0933.

Synthesis of 4-Methyl-2-(2-thiophene-3-yl-acetylamino]-pentanoic Acid Methyl Ester (4). Product: viscous pale yellow liquid. The solvent used for the column chromatography on silica gel was ethyl acetate/CH_2Cl_2 (40/50, R_f = 0.80). Yield: 75%. ^{1}H NMR (200 MHz, $CDCl_3$) δ (ppm) 7.78−7.32 (m 1H), 7.32−7.20 (m, 1H), 7.20−7.08 (m, 1H), 7.00−6.76 (m, 1H), 4.84−4.60 (m, 1H), 3.80 (s, 3H), 3.70 (s, 2H), 1.88−1.48 (m, 3H), 1.16−0.84 (m, 6H). ^{13}C NMR (50 MHz, $CDCl_3$) δ (ppm) 173.3, 170.5, 134.7, 128.4, 126.3, 123.1, 52.1, 50.8, 41.2, 37.8, 24.9, 22.8, 21.9. IR-(NaCl) υ (cm^{-1}) 1737 (CO ester), 1643 (CO amide). UV−vis (ACN) λ_{max} (ε) 261 nm (3.88×10^3 M^{-1} cm^{-1}). HRMS (EI) for $C_{13}H_{19}NO_3S$ [M^+]: calcd 269.1080; found 269.1085.

Synthesis of 4-Methyl-2-[(thiophene-3-carbonyl)-amino]-pentanoic Acid (5). Product: viscous white liquid. Yield: 95%.^{1}H NMR (200 MHz, DMSO-d_6) δ (ppm) 12.60 (s br, 1H), 8.40 (d, J = 7.8 Hz, 1H), 8.30−8.10 (m, 1H), 7.65−7.40 (m, 2H), 4.50−4.30 (m, 1H), 1.84−1.40 (m, 3H), 1.04−0.70 (m, 6H). ^{13}C NMR (50 MHz, DMSO-d_6) δ (ppm) 174.1, 162.0, 137.2, 128.9, 126.9, 126.5, 50.4, 24.4, 22.9, 21.1. IR(NaCl) υ (cm^{-1}) 1706 (CO carboxylic acid), 1610 (CO amide). UV−vis (ACN) λ_{max} (ε) 242 nm (1.06×10^4 M^{-1} cm^{-1}). HRMS (EI) for $C_{11}H_{15}NO_3S$ [M^+]: calcd 241.0767; found 241.0767.

Synthesis of 4-Methyl-2-(2-thiophen-3-yl-acetylamino)-pentanoic Acid (6). Product: white solid. Yield: 95%. Mp: 141 °C. ^{1}H NMR (200 MHz, DMSO-d_6) δ (ppm) 8.30 (d, J = 7.8 Hz, 1H), 7.50−7.40 (m, 1H), 7.30−7.20 (m, 1H), 7.10−6.95 (m, 1H), 4.30−4.10 (m, 1H), 3.45 (s, 2H), 1.70−1.40 (m, 3H), 1.00−0.75 (m, 6H). ^{13}C NMR (50 MHz, DMSO-d_6) δ (ppm) 174.0, 169.6, 136.0, 128.5, 125.4, 121.9, 50.3, 36.7, 24.3, 22.8, 21.3. IR (KBr) υ (cm^{-1}) 1699 (CO carboxylic acid), 1618 (CO amide). UV−vis (ACN) λ_{max} (ε) 235 nm (3.83×10^3 M^{-1} cm^{-1}). HRMS (EI) for $C_{12}H_{17}NO_3S$ [M^+]: calcd 255.0924; found 255.0925.

Synthesis of 2-[(2,5-Dibromo-thiophene-3-carbonyl)-amino]-4-methyl-pentanoic Acid Methyl Ester (9). Product: clear viscous liquid. The solvent used for the column chromatography on silica gel was ethyl acetate/CH_2Cl_2 (5/95, R_f = 0.62). Yield: 62%. ^{1}H NMR (200 MHz, $CDCl_3$) δ (ppm) 8.65 (d, J = 7.4 Hz, 1H), 7.45 (s, 1H), 4.50−4.30 (m, 1H), 3.64 (s, 3H), 1.90−1.40 (m, 3H), 1.00−0.80 (m, 6H). ^{13}C NMR (50 MHz, $CDCl_3$) δ (ppm) 172.4, 160.9, 136.3, 130.6, 113.6, 110.9, 51.8, 50.7, 24.2, 22.7, 21.0. IR(NaCl) υ (cm^{-1}) 1730 (CO ester), 1625 (CO amide). UV−vis (ACN) λ_{max} (ε) 256 nm (2.33×10^3 M^{-1} cm^{-1}). HRMS (EI) for $C_{12}H_{15}Br_2NO_3S$ [M^+]: calcd 410.9134; found 410.9137.

Synthesis of 2-[2-(2,5-Dibromo-thiophen-3-yl)-acetylamino]-4-methyl-pentanoic Acid Methyl Ester (10). Product: yellow viscous liquid. The solvent used for the column chromatography on silica gel was ethyl acetate/CH_2Cl_2 (10/90, R_f = 0.50). Yield: 64%. ^{1}H NMR (200 MHz, $CDCl_3$) δ (ppm) 8.55 (d, J = 7.4 Hz, 1H), 7.01 (s, 1H), 4.40−4.20 (m, 1H), 3.60 (s, 3H), 3.40 (s, 2H), 1.80−1.40 (m, 3H), 1.00−0.70 (m, 6H). ^{13}C NMR ($CDCl_3$) δ (ppm) 172.3, 168.1, 137.1, 132.3, 109.5, 109.2, 51.7, 50.4, 38.2, 35.4, 24.2, 22.6, 21.2. IR(NaCl) υ (cm^{-1}) 1728 (CO ester), 1645 (CO amide). UV−vis (ACN) λ_{max} (ε) 272 nm (3.12×10^3 M^{-1} cm^{-1}). HRMS (EI) for $C_{13}H_{17}Br_2NO_3S$ [M^+]: calcd 424.9290; found 424.9289.

Synthesis of 4-Methyl-2-[([2,2′;5′,2″]terthiophene-3′-carbonyl)-amino]-pentanoic Acid Methyl Ester (11). Product: orange viscous liquid. The solvent used for the column chromatography on silica gel was ethyl acetate/CH_2Cl_2 (10/90, R_f = 0.65). Yield: 50%. ^{1}H NMR (200 MHz, $CDCl_3$) δ (ppm) 7.40−6.76 (m, 7H), 6.04 (d, J = 8.2 Hz, 1H), 4.64−4.40 (m, 1H), 3.50 (s, 3H), 1.56−1.10 (m, 3H), 0.92−0.56 (m, 6H). ^{13}C NMR (50 MHz, $CDCl_3$) δ (ppm) 173.2, 163.2, 137.0, 136.1, 134.7, 134.5, 133.0, 129.5, 128.4, 128.1, 127.9, 125.6, 125.5, 124.7, 52.4, 51.2, 41.6, 24.9, 22.9, 22.1. IR (NaCl) υ (cm^{-1}) 1737 (CO ester), 1639 (CO amide). UV−vis

(ACN) λ_{max} (ε) 348 nm (1.63×10^4 M^{-1} cm^{-1}). HRMS (EI) for $C_{20}H_{21}NO_3S_3$ [M^+]: calcd 419.0678; found 419.0685.

Synthesis of 4-Methyl-2-(2-[2,2′;5′,2″]terthiophene-3′-yl)-acetylamino]-pentanoic Acid Methyl Ester (12). Product: yellow solid. The solvent used for the column chromatography on silica gel was ethyl acetate/CH_2Cl_2 (20/80, R_f = 0.80). Yield: 50%. Mp: 86 °C. ^{1}H NMR (200 MHz, $CDCl_3$) δ(ppm) 7.56−7.08 (m, 7H), 6.24 (d, J = 7.4 Hz, 1H), 4.92−4.68 (m, 1H), 3.93 (s, 2H), 3.92 (s, 3H), 1.90−1.50 (m, 3H), 1.20−0.90 (m, 6H). ^{13}C NMR (50 MHz, $CDCl_3$) δ (ppm) 173.2, 169.7, 136.7, 136.6, 134.7, 132.5, 131.5, 128.0, 127.9, 126.9, 126.7, 126.3, 125.0, 124.2, 52.3, 51.0, 41.4, 37.2, 25.0, 22.9, 22.0. IR (KBr) υ (cm^{-1}) 1741 (CO ester), 1647 (CO amide). UV−vis (ACN) λ_{max} (ε) 342 nm (1.62×10^4 M^{-1} cm^{-1}). HRMS (EI) for $C_{21}H_{23}NO_3S_3$ [M^+]: calcd 433.0835; found 433.0841.

Synthesis of 4-Methyl-2-[([2,2′;5′,2″]terthiophene-3′-carbonyl)-amino]-pentanoic Acid (13). Product: yellow solid. Yield: 95%. Mp: 77 °C. ^{1}H NMR (200 MHz, DMSO-d_6) δ (ppm) 8.65 (d, J = 7.8 Hz, 1H), 7.70−7.55 (m, 2H), 7.55−7.30 (m, 3H), 7.30−7.00 (m, 2H), 4.47−4.24 (m, 1H), 1.80−1.40 (m, 3H), 1.05−0.70 (m, 6H). ^{13}C NMR (50 MHz, DMSO-d_6) δ (ppm) 173.7, 163.6, 135.0, 134.7, 134.2, 133.5, 133.4, 128.4, 127.7, 127.6, 126.2, 124.8, 50.7, 24.3, 22.8, 21.2. IR (KBr) υ (cm^{-1}) 1716 (CO carboxylic acid), 1635 (CO amide). UV−vis (ACN) λ_{max} (ε) 344 nm (1.17×10^4 M^{-1} cm^{-1}). HRMS (EI) for $C_{19}H_{19}NO_3S_3$ [M^+]: calcd 405.0522; found 405.0535.

Synthesis of 4-Methyl-2-(2-[2,2′;5′,2″]terthiophen-3′-yl-acetyl-amino)-pentanoic Acid (14). Product: orange solid. Yield: 94%. Mp: 102 °C. ^{1}H NMR (200 MHz, DMSO-d_6) δ (ppm) 8.02 (d, J = 7.0 Hz, 1H), 7.72−7.60 (m, 1H), 7.60−7.48 (m, 1H), 7.48−7.36 (m, 1H), 7.36−7.22 (m, 2H), 7.22−7.02 (m, 2H), 4.20−3.96 (m, 1H), 3.59 (s, 2H), 1.80−1.30 (m, 3H), 1.00−0.70 (m, 6H). ^{13}C NMR (50 MHz, DMSO-d_6) δ (ppm) 174.1, 168.5, 135.9, 134.3, 133.9, 133.5, 130.4, 128.3, 128.1, 127.4, 126.6, 126.5, 125.6, 124.0, 51.5, 37.9, 35.9, 24.4, 23.0, 21.7. IR (KBr) υ (cm^{-1}) 1716 (CO carboxylic acid), 1649 (CO amide). UV−vis (ACN) λ_{max} (ε) 342 nm (1.12×10^4 M^{-1} cm^{-1}). HRMS (EI) for $C_{20}H_{21}NO_3S_3$ [M^+]: calcd 419.0678; found 419.0682.

Acknowledgment. M.C. thanks Laurentian University and the Natural Science and Engineering Research Council of Canada (NSERC) for supporting this work.

Supporting Information Available: ^{1}H and ^{13}C NMR spectra of **3**−**6** and **9**−**14**; electropolymerization of terthiophene; ATR-IR of poly(**11**−**14**)-*Pt*; CVs of the interactions of poly-(**14**)-*Pt* with D-leucine methy ester, D/L-leucine methyl ester, D-alanine methyl ester, and L-alanine methyl ester; and ^{1}H NMR spectra of **6** in the presence of D-leucine methyl ester and D/L-leucine methyl ester. This material is available free of charge via the Internet at http://pubs.acs.org.